European Polymer Journal 44 (2008) 3754–3763

Contents lists available at ScienceDirect

European Polymer Journal

journal homepage: www.elsevier.com/locate/europolj

Effects of polyamide 6 on the crystallization and melting behavior of β-nucleated polypropylene

Zhugen Yang, Zishou Zhang, Youji Tao, Kancheng Mai *

Materials Science Institute, School of Chemistry and Chemical Engineering, Sun Yat-Sen University, Key Laboratory of Polymeric Composites and Functional Materials of the Ministry of Education, Guangzhou 510275, People's Republic of China

ARTICLE INFO

Article history:
Received 4 May 2008
Received in revised form 13 August 2008
Accepted 15 August 2008
Available online 26 August 2008

Keywords:
β-polypropylene
Polyamide 6
Crystallization behavior
Melting characteristic

ABSTRACT

Non-nucleated polypropylene alloy with polyamide 6 (PP/PA6) and β-nucleated polypropylene (β-PP)/PA6 alloy, as well as its compatibilized version with maleic anhydride grafted PP (PP-*g*-MA) were prepared with an internal mixer. In the all alloys, PP formed a continuous phase with a dispersive PA6. Effects of PA6 on the non-isothermal crystallization behavior, melting characteristics and the β-PP content of alloys were investigated by differential scanning calorimeter (DSC) and wide angle X-ray diffraction (WAXD). The results indicated that the crystallization temperature (T_c^p) of PP shifts to high temperature in the non-nucleated PP/PA6 alloys due to the α-nucleating effect of PA6. However, in the β-nucleated PP/PA6 alloys, PA6 hardly has an effect on the T_c^p of PP. The β-PP content in the alloys not only depends on the content of the PA6, but also on the melting temperatures. It is proved by etching the alloys with sulfuric acid that the nucleating agent mainly disperses in the PA6 phase and/or the interface between PP and PA6 when blended at high temperature. Addition of PP-*g*-MA promotes the formation of β-PP in the β-nucleated PP/PA6 alloys. The increase in the PA6 content has a little influence on the T_c^p of PP and the β-PP content in the compatibilized β-nucleated PP/PA6 alloys. The non-isothermal crystallization kinetics of PP in the alloys was evaluated by Mo's method.

1. Introduction

Isotactic polypropylene (PP) is a polymorphic material with three known possible crystal forms, namely, monoclinic (α-PP), trigonal (β-PP), and triclinic (γ-PP) [1,2]. The metastable β-PP has attracted interest because β-PP has unusual performance characteristic, including improved elongation at break, impact strength and higher heat distortion temperature [3–5]. High content of β-PP can be obtained under special crystallization conditions such as the introduction of a β-nucleating agent [6–9], a temperature gradient [10–11] and shearing or elongation of the melt [12–15]. However, the yield strength and elastic modulus of β-PP are lower than those of α-PP. In order to improve the properties of β-PP, β-PP blending with other polymers shall be become an increasingly important method.

More attentions were focused on the stability of β-PP in its blends because the β-PP may easily transfer to α-PP due to the effect of the second component. Zhang et al. [16] studied the β to α transformation of PP in compatibilized PP/PA6 blend. It was observed that the β to α transformation could only be activated at elevated tensile testing temperatures in β-nucleated PP/PA6 blends compatibilized by PP-*g*-MA. It is attributed to the increase in tensile elongation at break with increasing the tensile testing temperature. Besides, the presence of PA6 particles in the predominantly β-PP matrix has no influence on the β to α transformation. Feng et al. [17] suggested that the shear flow field during cavity filling plays an important role in the formation of β-PP in the blends of PP and polyamide 6/clay nanocomposites (PP/NPA6). It is attributed that the increased clay content reduces the domain deformation

* Corresponding author. Tel./fax: +86 20 84115109.
E-mail addresses: cesmkc@mail.sysu.edu.cn, cesmkc@zsu.edu.cn (K. Mai).

0014-3057/$ - see front matter © 2008 Elsevier Ltd. All rights reserved.
doi:10.1016/j.eurpolymj.2008.08.010

(the dispersed NPA6 phase), thereby enhancing the shear between the NPA6 phase and the PP matrix, which leads to the formation of β-PP under proper crystallization conditions in the mold. He also found that the introduction of NPA6 rather than PA6 in blends with PP induced significant β-PP during injection molding. However, the formation mechanism involved in the process is needed to better understand.

It has been observed that β-PP based polymer blends can be prepared without any difficulty if the second component is amorphous e.g., elastomer [18–20]. However, PP matrix crystallized predominantly in α-PP in the presence of the second component with α-nucleating ability, such as poly(vinylidene-fluoride) (PVDF) and PA6 [21,22]. Menyhárd et al. [22] suggested that the most important factor of the formation a blend with β-PP is the α-nucleation effect of the second component. If the T_c^p of the second component with α-nucleating effect is lower than that of PP, addition of the second component has little influence on the formation of β-PP. On the contrary, if the T_c^p of the second component with α-nucleating effect is higher than that of PP, addition of the second component suppresses the formation of β-PP. e.g., in the β-nucleated PP/PVDF and PP/PA6 blends, the β-PP can not form even in the presence of a highly effective β-nucleated agent due to the strong α-nucleating ability and higher T_c^p of PVDF and PA6. Menyhárd et al. [23] also concluded that a PP matrix consisting mainly of the α-PP was formed already at low PA6 content in the non-compatibilized β-nucleated PP/PA6 blends. On the contrary, predominantly β-PP matrix developed in the presence of maleic anhydride grafted PP (PP-*g*-MA) compatibilizer. The formation of α-PP matrix in the absence of compatibilizer is related to the selective encapsulation of β-nucleating agent in the polar PA6 phase. However, this explanation is needed to be proved by further experimental facts.

Although the β-PP alloys have been investigated, the distribution of nucleating agents in the different phases is still an open question in general. Only a few studies have been reported on this topic [24,25] and references therein. As a consequence the main goal of this study was to clear this point adequately. In the paper, non- and β-nucleated PP/PA6 alloys was prepared with addition of a highly efficient nano-$CaCO_3$ supported β-nucleating agent, with PP-*g*-MA as a compatibilizer. Effects of PA6 on the non-isothermal crystallization behavior, melting characteristics and the β-PP content of the alloys were investigated by differential scanning calorimeter (DSC) and wide angle X-ray diffraction (WAXD). Additionally, we try to prove the hypothesis that the nucleating agents mainly disperse in the PA6 phase and/or the interface between PP and PA6 in the process of mixing at high temperature by etching the alloys with sulfuric acid. Non-isothermal crystallization kinetics was analyzed using theoretical method proposed by Mo and co-workers.

2. Experimental

2.1. Materials

Isotactic polypropylene (PP, HP500N) was homopolymer grade, supplied by CNOOC and Shell Petrochemicals Co., Ltd., MFR = 12 g/10 min (230 °C, 2.16 kg). Polyamide 6 (PA6, Grade M2800) has a relative viscosity of 2.83, supplied by Guangdong Xinhui Media Nylon Co., Ltd., MFR = 11 g/10 min (230 °C, 2.16 kg). Maleic anhydride grafted PP (PP-*g*-MA) was commercial products, supplied by Guangzhou Lushan Chemical Materials Co., Ltd., the grafted contents of MA was 1.0. Active nano-$CaCO_3$ was obtained from Gavin Chemical Industrial Enterprise Co., Ltd., of Guangdong Province in China. Aliphatic dicarboxylic acid was supplied by Shanghai Hongsheng Industry Co., Ltd., whose purity is 98%. Sulfuric acid (H_2SO_4), analytical reagent (AR), was obtained from Guangzhou Chemical Reagent Factory, whose content was 95–98 wt%. Potassium carbonate (K_2CO_3), AR, was supplied by Tianjin Damao Chemical Reagent Factory.

2.2. Specimen preparation

Before blending, all the materials were adequately dried in a vacuum oven at appropriate temperatures for 12 h. The nano-$CaCO_3$ supported β-nucleating agent was prepared from aliphatic dicarboxylic acid and nano-$CaCO_3$ (wt/wt, 1/50) in our lab. 5 wt% nano-$CaCO_3$ supported β-nucleating agents were added to PP to prepare β-nucleated PP on a Berstoff ZE25A corotating twin-screw extruder (L/D = 40, D = 35.5 mm) at 200 °C with the screw rotation of 480 rpm and residue time of 40 s. Extrudates were cooled in a water bath and cut into pellets by a pelletizer.

The non- and β-nucleated PP/PA6 alloys were prepared using an internal mixer (Rheocord 300p, Germany) at 240 °C and 50 rpm, mixed for 8 min. In the same case, the PP-*g*-MA (5 phr) was added to prepare the compatibilized β-nucleated PP/PA6 alloys. In the binary alloys, the amount of PA6 was 10, 20, 30 and 40 wt%. All the alloys composed of various compositions were shown in Table 1.

Small thin pieces cut from β-nucleated PP/PA6 alloys were dipped into the sulfuric acid for 24 h to etch the PA6 component. The alloy was dried in a vacuum oven at 80 °C for 12 h for DSC measurements after washed with the potassium carbonate solution and large amount of distilled water in the order.

2.3. Differential scanning calorimeter (DSC)

DSC measurements were made on a TA DSC Q10 differential scanning calorimeter (DSC), the temperature calibrated with indium in nitrogen atmosphere. About 5 mg sample was weighted very accurately. It was heated to 260 °C with 40 °C/min, held there for 5 min, and then cooled to 100 °C with cooling rate of 10 °C/min. This controlled cooling temperature prevents β–α transformation [6], so the polymorphic composition of the sample can be determined accurately for the melting curves [1,23]. The sample was reheating to 260 °C with the heating rate of 10 °C/min for melting behavior study. For the effect of melting temperature, the only alloy was first pre-melting at the temperature of 180 °C for 5 min and then cooled to 100 °C at the cooling rate of 10 °C/min, reheating to 180 °C at the heating rate of 10 °C/min. Repeat the procedure but the melting temperature turned to 200, 220, 220, 240, 260, 280, 260, 240, 220, 200 and 180 °C as the or-

Table 1
DSC data of PP and PA6 component in PP/PA6 alloys*

Samples		T_c^p (°C)		$-\Delta H_c$ (J/g)		T_m^p (°C)			ΔH_m (J/g)			Φ_β (%)
		PP	PA6	PP	PA6	β-PP	α-PP	PA6	β-PP	α-PP	PA6	
PP/PA6	100/0	112.6	–	101.7	–	–	160.2	–	–	103.1	–	–
	90/10	121.7	185.9	108.9	9.3	–	162.5	220.0	–	110.8	59.0	–
	80/20	122.1	187.4	102.9	45.5	–	162.6	220.4	–	101.0	61.5	–
	70/30	122.4	187.8	100.8	60.3	–	162.7	220.4	–	99.7	54.7	–
	60/40	121.7	187.9	103.5	70.8	–	162.5	220.4	–	99.0	58.0	–
	0/100	–	186.6	–	76.4	–	–	220.7	–	–	79.8	–
β-PP/PA6	100/0	124.3	–	87.4	–	150.7	163.1	–	82.4	2.7	–	97.0
	90/10	123.3	186.4	89.0	46.0	150.2	162.7	220.0	76.4	4.5	47.0	94.7
	80/20	123.1	189.6	91.8	69.0	149.5	162.4	220.1	60.3	32.8	57.0	65.6
	70/30	123.1	190.7	97.7	71.3	149.0	162.1	220.1	46.9	50.3	57.3	35.6
	60/40	122.2	190.4	94.8	70.8	149.3	162.6	220.4	27.7	64.5	57.5	15.8
Etched β-PP/PA6	100/0	123.4	–	91.2	–	149.2	161.7		84.9	3.1	–	96.6
	90/10	120.2	–	93.2	–	–	161.6	–	–	93.1	–	–
	80/20	119.4	–	95.3	–	–	161.3	–	–	94.3	–	–
	70/30	119.5	–	94.3	–	–	161.2	–	–	93.5	–	–
	60/40	119.2	187.7	89.3	2.2	–	161.6	218.6	–	90.2	1.9	–
5 phr PP-*g*-MA	90/10	123.6	185.3	91.3	7.7	149.1	161.6	219.0	80.4	4.3	53.0	95.1
	80/20	122.9	185.6	93.3	8.5	149.7	162.1	219.5	78.0	5.7	57.0	90.6
	70/30	123.4	186.2	95.7	8.7	148.6	161.4	219.2	73.6	16.3	70.0	85.1
	60/40	122.9	186.1	92.5	6.0	148.8	161.6	218.8	71.2	17.8	69.3	81.6

* T_c^p, temperature of crystallization peak; T_m^p, temperature of melting peak; ΔH_c, enthalpy of crystallization; ΔH_m, enthalpy of fusion; Φ_β, the percentage of β-phase calculated according to DSC.

der. The crystallization and melting parameters were recorded from the cooling and reheating scans. The percentage of β-phase, Φ_β, can be obtained according to Ref. [26].

2.4. Wide angle X-ray diffraction (WAXD)

The wide angle X-ray diffraction (WAXD) patterns of the samples were recorded at room temperature using a Rigaku D/Max 2200 unit equipped with Ni-filtered Cu–Ka radiation in the reflection mode with a wavelength of 0.154 nm. For direct comparison, the specimens were prepared on TA DSC Q10 thermal system under the condition, where heated to 260 °C with 40 °C/min, held there for 5 min, and then cooled to 40 °C with cooling rate of 10 °C/min. The operating condition of the X-ray source was set at a voltage of 40 kV and a current of 30 mA in a range of $2\theta = 5–40°$ with a step scanning rate of 2°/min.

3. Results and discussion

3.1. The effect of PA6 content on non-nucleated PP/PA6 alloys

The DSC cooling and heating curves of non-nucleated PP/PA6 alloys with various PA6 contents are shown in Fig. 1, and the crystallization and melting parameters are listed in Table 1. As is shown in Fig. 1a, the crystallization peaks appearing in the vicinity of 120 °C and 190 °C are attributed to the crystallization of PP and PA6, respectively. It can be seen that the intensity of the crystallization peak of PP became weaker with increasing the PA6 content, in addition, the peak of PA6 was present and its intensity became stronger. It can be observed from Fig. 1b that a tiny melting peak of β-PP at round 150 °C appears in neat PP. However, in the non-nucleated PP/PA6 alloys, the sole melting peak of α-PP was observed and its intensity also became weaker with increasing the PA6 content. Double melting peaks at about 220 °C are attributed to the melting of PA6 in non-nucleated PP/PA6 alloys.

As is shown in Table 1, the crystallization temperature (T_c^p) of neat PP is 112.6 °C, but addition of 10 wt% PA6 increases the T_c^p of PP to 121.7 °C. It suggests that PA6 has α-nucleating effect on the crystallization of PP, which promotes the formation of a matrix rich in α-PP and increases its T_c^p. However, the increase in the PA6 content has a little effect on the T_c^p of PP in the alloys [21–23]. It can be also observed from Fig. 1 that the T_c^p of PA6 shifts to high temperature in the presence of PP. These results indicate that the PA6 crystallizes more easily in the presence of molten PP.

3.2. The effect of PA6 content on the β-nucleated PP/PA6 alloys

The DSC cooling and heating curves of β-nucleated PP/PA6 alloys with various PA6 contents are shown in Fig. 2 and the crystallization and melting parameters are listed in Table 1. It can be seen that the crystallization behavior of PP in β-nucleated PP/PA6 alloys is quite different from that in non-nucleated PP/PA6 alloys. Firstly, the T_c^p of β-nucleated PP (124.3 °C) is much higher than that of non-nucleated PP (112.6 °C). Addition of PA6 decreases the T_c^p of PP in the β-nucleated PP. However, addition of PA6 increases the T_c^p of PP in the non-nucleated PP. Secondly, the increase in the PA6 content decreases the T_c^p of PP in β-nucleated PP/PA6, but the increase in the PA6 content increases the T_c^p of PP in non-nucleated PP/PA6. In addition, the T_c^p of PP in β-nucleated PP/PA6 alloys containing 40 wt% PA6 is almost the same with that in

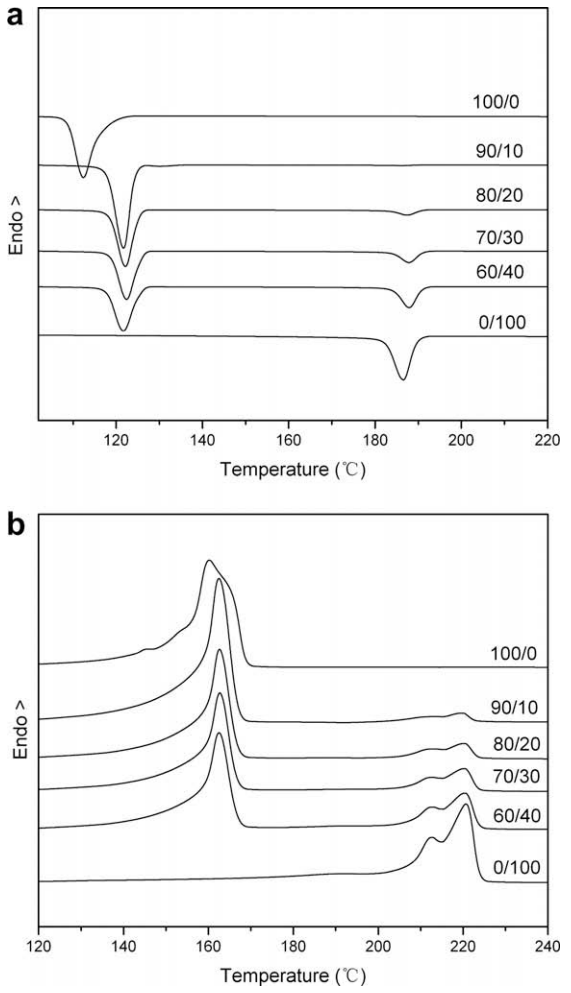

Fig. 1. DSC cooling (a) and heating (b) curves of non nucleated PP/PA6 alloys with various contents of PA6.

non-nucleated PP/PA6 with the same component. It can be suggested that there is a competition between the selective encapsulation of the nucleating agents and the α-nucleating effect of PA6 in β-nucleated PP/PA6 alloys. In the preparation process of alloys, the β-nucleating agent in PP might move to PA6 phase and/or the interface between PP and PA6 due to the interaction between the polar groups of β-nucleating agent and the polar groups of PA6. This interaction decreased the concentration of β-nucleating agent in PP matrix and resulted in the decrease in the nucleation effect of β-nucleating agent and the T_c^p of PP. For the alloys with high PA6 content, the β-nucleating agent was almost encapsulated in PA6 phase and the PA6 played a strong α-nucleating effect on PP crystallize. Therefore, the T_c^p of PP in β-nucleated PP/PA6 alloy is almost the same as that in the non-nucleated PP/PA6 alloys containing 30–40 wt% PA6.

For the β-nucleated PP/PA6 alloy, the increase in the T_c^p of PA6 is also observed in the presence of molten PP. The T_c^p of PA6 shifts from 186.6 °C of neat PA6 to 190.7 °C in the alloy containing 30 wt% PA6. It is also indicated that the PA6 crystallizes more easily in the presence of molten PP. The more pronounced increase of T_c^p of PA6 in the case of β-nucleated alloys suggests that the nucleating agent may have nucleating effect on PA6 as well. Moreover, the steeper increase of T_c^p in the case of β-nucleated alloys is a further proof for the encapsulation of the β-nucleating agent.

The WAXD spectra of β-nucleated PP/PA6 alloys with different PA6 contents are shown in Fig. 3. It can be observed that the PP exhibited α-crystallization form appeared at $2\theta = 14.3°$, 16.8° and 18.6°, corresponding to the plane (110), (040) and (130) of α-PP. The reflection at $2\theta = 16.1°$ was corresponding to the plane (300) of the β-PP [13,14]. The only diffraction peak of α-PP and β-PP were observed in the non-nucleated PP and β-nucleated PP, respectively. However, the intensity of the diffraction peak of β-PP decreased and that of α-PP increased with increasing the PA6 content in the β-nucleated PP/PA6 alloys. The diffraction peak of the plane (300) of β-PP almost disappeared in the β-nucleated PP/PA6 alloy containing 40 wt% PA6.

The relative β-PP content (K_β) was calculated according to the equation suggested by Turner-Jones: [27]

$$K_\beta = \frac{I_{\beta 1}}{I_{\beta 1} + I_{\alpha 1} + I_{\alpha 2} + I_{\alpha 3}} \quad (1)$$

Where $I_{\beta 1}$ is the diffraction intensity of β (300) plane, $I_{\alpha 1}$, $I_{\alpha 2}$ and $I_{\alpha 3}$ are the diffraction intensity of α (110), α (040) and α (130) plane, respectively. According to Eq. (1), the β-PP content in β-nucleated PP, the β-nucleated PP/PA6 alloys containing 10, 20, 30 and 40 wt% PA6 was as follow: 0.971, 0.932, 0.701, 0.342 and 0.176, respectively. It can be concluded that the results of the β-PP content obtained from WAXD were similar with those from DSC.

The DSC cooling and heating curves of β-nucleated PP/PA6 alloys with various contents of PA6 etched with sulfuric acid for 24 h at room temperature are shown in Fig. 4 and the crystallization and melting parameters are also listed in Table 1. It can be seen from Fig. 4a and Table 1 that the T_c^p of PP in β-nucleated PP was hardly influenced by etching with sulfuric acid and the β-PP content almost kept constant, which was 97.0% and 96.6% before and after etched with sulfuric acid, respectively. It can be concluded that the nucleating agent dispersed in PP phase can not be etched by sulfuric acid. However, for the β-nucleated PP/PA6 alloys etched with sulfuric acid, the crystallization and melting peak of PA6 almost disappeared. It is indicated that the PA6 phase was almost completely etched by sulfuric acid in β-nucleated PP/PA6 alloys. The T_c^p of PP in β-nucleated PP/PA6 alloys shifted to low temperature and decreased with increasing the PA6 content in the alloys etched by sulfuric acid, e.g., the T_c^p of PP decreased from 123.3 °C to 120.2 °C in the β-nucleated PP/PA6 alloy containing 10 wt% PA6.

The β-PP content was 94.7% in β-nucleated PP/PA6 alloy containing 10 wt% PA6 without etching, but there was only a melting peak at round 160 °C relative to α-PP in the DSC heating curve (Fig. 4b). It is attributed to that the nucleating agents distributed in the PP phase can not be etched due to the protection of the acid-resistant PP. However,

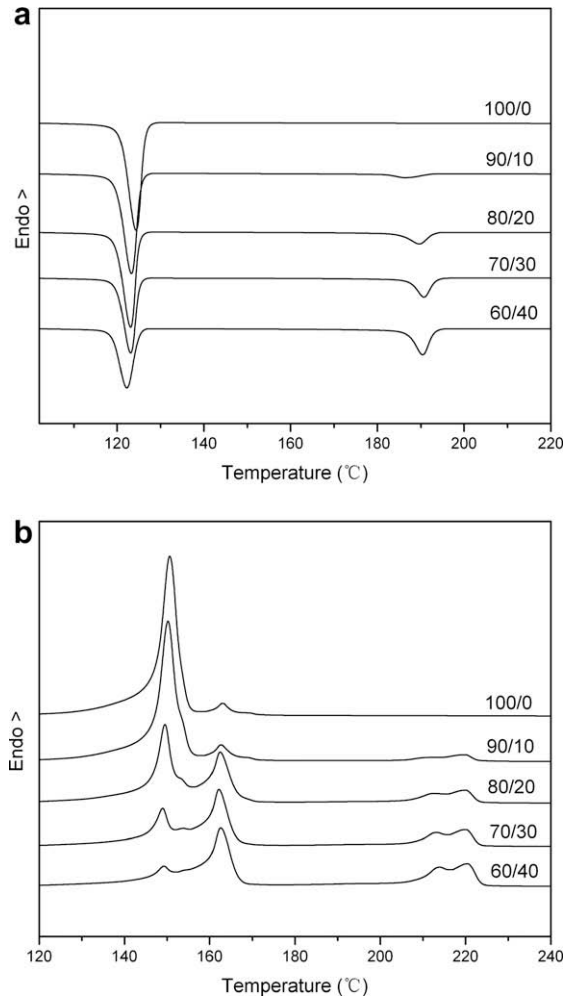

Fig. 2. DSC cooling (a) and heating (b) curves of β-nucleated PP/PA6 alloys with various contents of PA6.

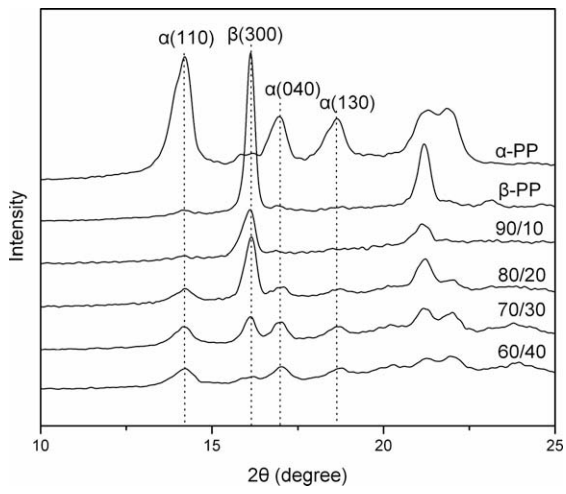

Fig. 3. X-ray spectra of non-nucleated PP, β-nucleated PP and β-nucleated PP/PA6 alloys.

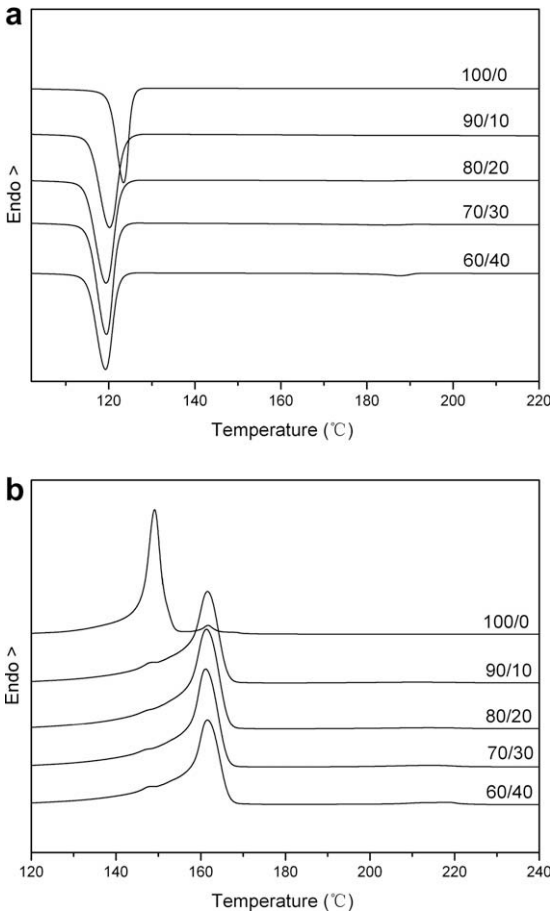

Fig. 4. DSC cooling (a) and heating (b) curves of β-nucleated PP/PA6 alloys with various contents of PA6 etched with sulfuric acid for 24 h.

PA6 could be easily etched by sulfuric acid and the exposed nucleating agents may also react with sulfuric acid, which results in the β-nucleating ability missing and the formation of a matrix rich in α-PP in the alloys. In conclusion, it has been proved that the β-nucleating agent can move to PA6 phase and/or the interface between PP and PA6 due to the polar interaction in the mixing process at high temperature.

3.3. The effect of PA6 content on compatibilized β-PP/PA6 alloys

The DSC cooling and heating curves of β-nucleated PP/PA6 (80/20) alloys compatibilized with PP-*g*-MA (5 phr) containing various contents of PA6 are shown in Fig. 5 and the crystallization and melting data are also listed in Table 1.

It can be seen from Fig. 5a that the T_c^p of PP was influenced slightly by the PA6 content in the alloys compatibilized with PP-*g*-MA, and the intensity of PA6 crystallization peak became weaker obviously compared to the uncompatibilized alloys. Although a tiny peak was observed at about 150 °C in the compatibilized alloys containing high content of PA6, the intensity of peak obviously decreased.

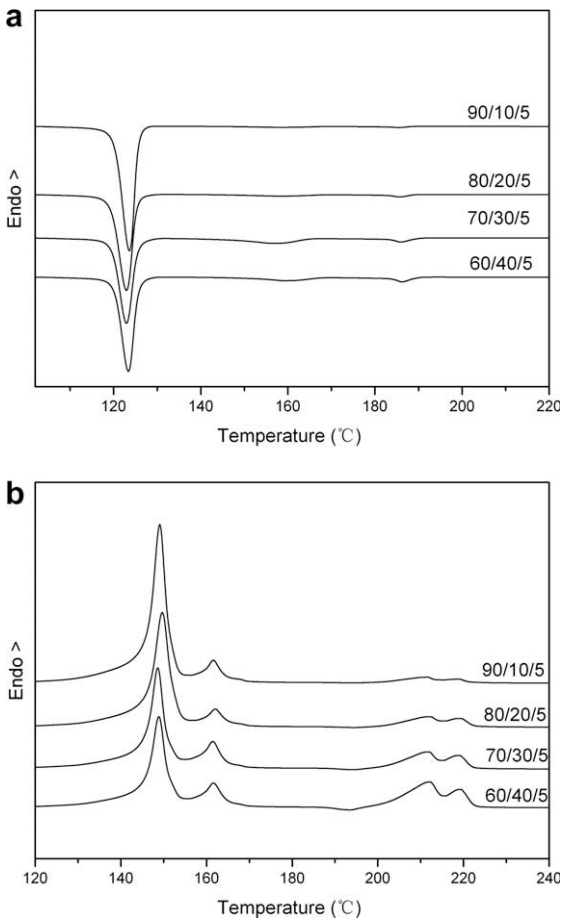

Fig. 5. DSC cooling (a) and heating (b) curves of β-nucleated PP/PA6/PP-*g*-MA alloys with various contents of PA6.

It can be observed from Fig. 5b and Fig. 2b that the intensity of β-PP melting peak in compatibilized alloy was stronger than that in uncompatibilized one. In addition, the β-PP content in the uncompatibilized alloys decreased more obviously than that in the compatibilized with increasing the PA6 content. It is suggested that addition of PP-*g*-MA increased the homogeneity of PA6 phase dispersion in the PP matrix with a reduction in the size of the domains and PP-*g*-PA copolymer formation at the interface, which also made the crystallinity of PA6 reduced [28,29]. On the other hand, addition of PP-*g*-MA suppressed the distribution of β-nucleating agent into PA6 phase [23]. As a result, the matrix rich in β-PP was formed in the compatibilized alloy.

According to Table 1 and the results form WAXD, the β-PP content (Φ_β) for β-nucleated PP/PA6 alloys determined by DSC almost has no discrepancy with the K_β value according to Turner-Jones. It can also been seen from Fig. 1b and Fig. 2b that the melting characteristics are quite different between non- and β-nucleated PP/PA6 alloys. Although the melting peak of PA6 became more intensive and the double peaks were observed with increasing the PA6 content in both alloys, the intensity of β-PP melting peak gradually decreased and the intensity of α-PP melting peak gradually increased with increasing the PA6 content. The β-PP content reduced from 94.7% to 15.8% when the weight percentage of PA6 changed from 10 wt% to 40 wt% in the alloys. The relationship of β-PP content (Φ_β) with the PA6 content in the β-nucleated PP/PA6 alloys is present in Fig. 6. It is suggested that the factors that decreased the β-PP content in the β-nucleated PP/PA6 alloys as follow: (1) Addition of PA6 promoted the formation of α-PP due to the α-nucleating ability of PA6. (2) The increase in the PA6 content increased the α-nucleating ability and made the β-nucleating agent easily move to PA6 phase and/or the interface between PP and PA6, resulting in the decrease in the efficient component of β-nucleating agent in PP phase.

3.4. The effect of melting temperature

The DSC cooling and heating curves of uncompatibilized β-nucleated PP/PA6 (80/20) alloy melted at various temperatures are shown in Fig. 7 and the crystallization and melting data are shown in Table 2.

It can be observed from Fig. 7a and Table 2 that the T_c^p of PP in the uncompatibilized alloy melted at below 220 °C was higher than that melted at above 220 °C when scanning from low temperature to high. The T_c^p of PP increased with increasing the melting temperature (T_{melt}) in the uncompatibilized alloy melted at below 220 °C. However, the results were just opposite when melted at above 220 °C. The T_c^p of PP in the uncompatibilized alloy decreased with increasing the T_{melt}. As is shown in Fig. 7b that the intensity of α-PP melting peak was much more intensive than that of β-PP and the intensity of β-PP decreased with increasing the T_{melt} for the alloy melted at below 220 °C. However, the intensity of β-PP melting peak became much more intensive for the alloy melted at 240–280 °C. In addition, the results obtained from scanning from high to low T_{melt} were similar with that from low to high T_{melt}. The reason for the higher T_c^p is the presence of remaining self nuclei in PP because of the low final temperature of heating run and self-nucleation occurred

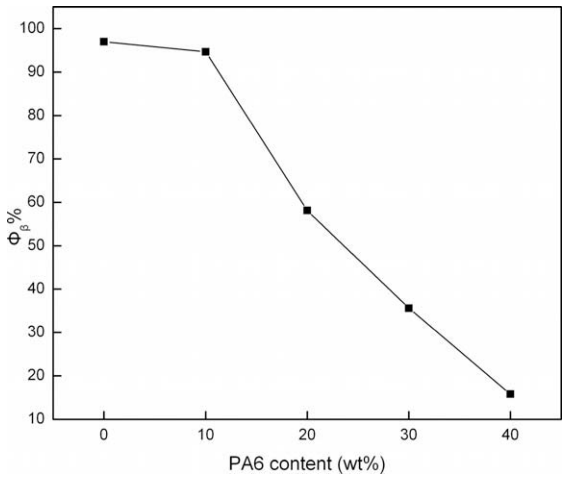

Fig. 6. Relationship of β-PP content (Φ_β) with PA6 content for β-nucleated PP/PA 6 alloys.

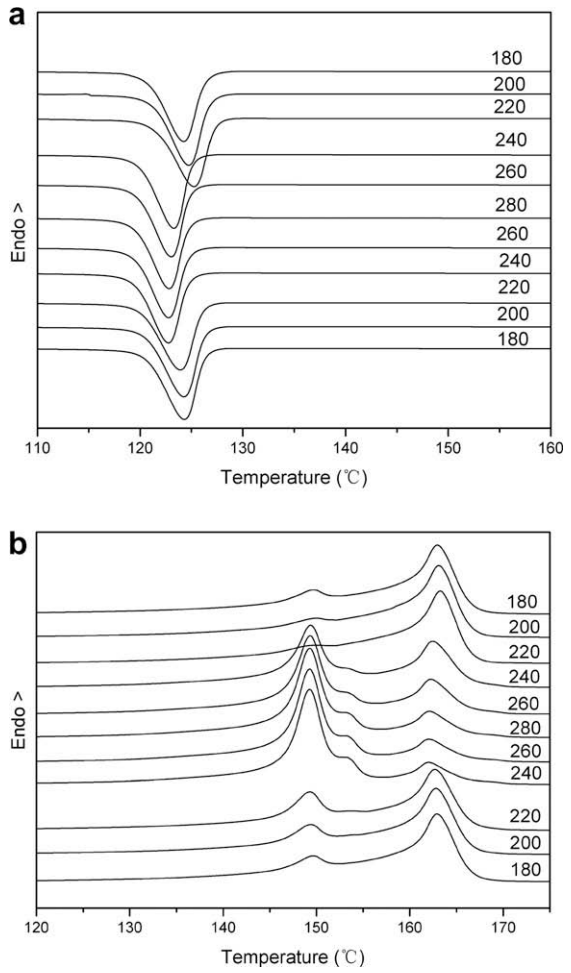

Fig. 7. DSC cooling (a) and heating (b) curves of β-nucleated PP/PA6 80/20 alloy melted at various temperatures as the order marked in the curve.

during the cooling process [30]. In addition, the PA6 was not melted but annealed to form high perfection crystals when the alloy was melted at below 220 °C, which resulted in the higher α-nucleating effect of PA6 to form a matrix rich in α-PP.

Fig. 8 illustrates the WAXD spectra of β-nucleated PP/PA6 alloys melted at various temperatures. The intensity of the diffraction peak of α-PP decreased and that of β-PP increased with increasing the T_{melt}. The β-PP content was calculated according to Eq. (1) and also listed in Table 2. It can be seen that the β-PP content increased with increasing the T_{melt} for the alloy melted at 180–280 °C. However, this conclusion was a little different from that obtained from DSC. It is attributed to that the alloy tested on WAXD was not melted at below PA6 melting point repeatedly but held at different T_{melt} for 5 min on DSC, respectively.

The influence of T_{melt} on the DSC curves of β-nucleated PP/PA6 (80/20) alloy compatibilized with PP-*g*-MA (5 phr) is presented in Fig. 9. Although the β-PP content in the compatibilized alloy is much higher than that in the uncompatibilized, the effect of T_{melt} on crystallization behavior and melting characteristic of the compatibilized alloy is similar with that of the uncompatibilized. The T_c^p of PP is higher and the matrix rich in α-PP is formed for the compatibilized alloy melted at below 220 °C. For the compatibilized alloy melted at above 220 °C, the T_c^p of PP shifts to low temperature and the matrix predominantly crystallize in β-form.

In conclusion, the β-PP content in the compatibilized β-nucleated PP/PA6 alloy is much dependent of the melting temperature. At the T_{melt} below 220 °C, PA6 phase is not melted but annealed to crystallize more perfectly. The annealed crystallized PA6 increases the α-nucleating ability of PA6 for PP crystallization, resulting in the formation of α-PP. At the T_{melt} above 220 °C, both PP and PA6 phase are in molten state and the β-nucleating ability of β-nucleating agent is higher than α-nucleating ability of PA6, which promotes the formation of a matrix rich in β-PP.

It is suggested that the β-PP content in the β-nucleated PP/PA6 alloy is relative to the factors as follow: (1) the α-nucleating effect of PA6 for PP crystallization is relative to the crystallinity of PA6. The more perfectly PA6 crystals, the higher of α-nucleating ability is. (2) The nucleation ability of β-nucleating agent is higher than that of α-nucleating ability of PA6 for the alloy melted at above the melting point of PA6. (3) The nucleation ability of β-nucleating agent is also influenced by the

Table 2
DSC data of PP component in β-nucleated PP/PA680/20 alloy melted at various temperatures

T_{melt} (°C)	T_c^p (°C)	T_c^{on} (°C)	$-\Delta H_c$ (J/g)	T_m^p (°C)		T_m^{on} (°C)		ΔH_m (J/g)		Φ_β (%)	K_β
				β	α	β	α	β	α		
180	124.2	126.4	97.4	149.7	162.9	144.1	159.0	31.1	65.4	14.5	0.176
200	124.8	126.8	96.0	149.7	162.9	143.6	159.0	26.9	70.0	–	0.263
220	125.3	127.3	98.8	150.0	163.1	141.7	159.0	28.1	70.1	–	0.305
240	123.3	125.0	94.3	150.1	163.3	141.3	159.2	58.9	38.0	53.5	0.592
260	123.0	124.9	93.3	149.4	162.4	146.1	159.0	69.5	27.4	66.7	0.701
280	122.8	124.7	92.4	149.3	162.2	146.2	159.0	76.5	20.1	75.8	0.806
260	122.8	124.7	91.9	149.3	162.1	146.2	158.9	78.8	17.0	69.2	0.701
240	122.8	124.7	91.8	149.3	162.0	146.2	158.9	80.5	16.6	54.3	0.592
220	123.9	126.1	97.4	149.3	162.0	146.2	158.9	47.5	50.8	33.1	0.305
200	124.3	126.3	98.5	149.3	162.7	144.9	158.6	40.1	57.9	22.0	0.263
180	124.3	126.3	98.3	149.4	162.8	144.3	158.7	31.8	64.1	16.7	0.176

K_β, the value representing β-content calculated according to WAXD.

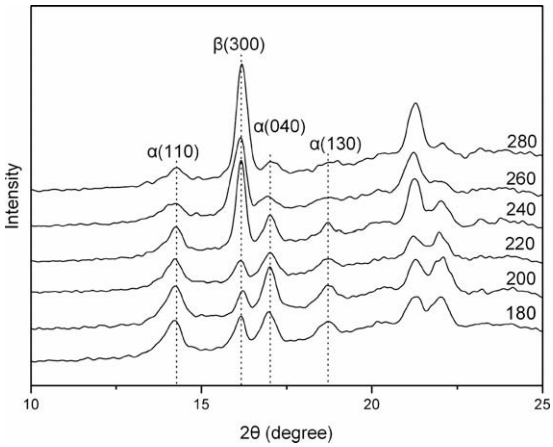

Fig. 8. X-ray spectra of β-nucleated PP/PA6 80/20 alloy melted at various temperatures.

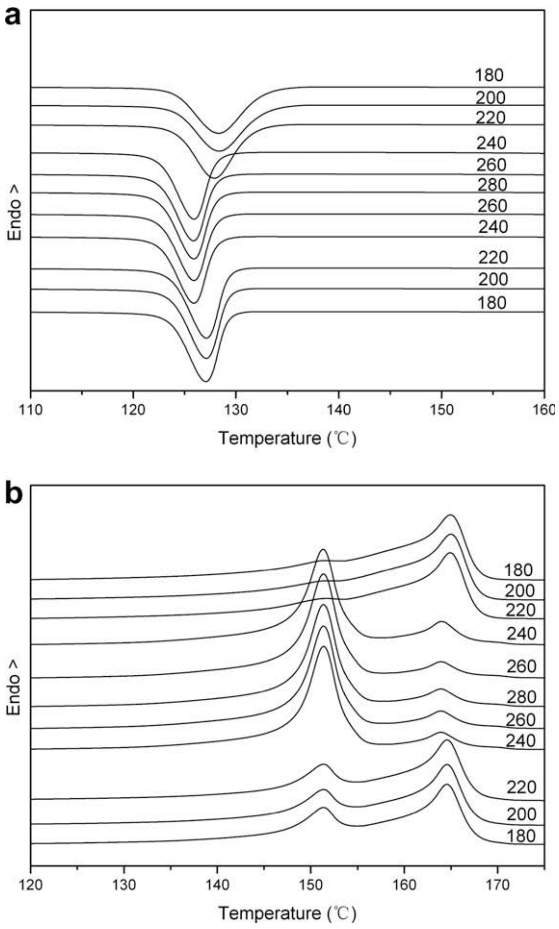

Fig. 9. DSC cooling (a) and heating (b) curves of compatibilized β-nucleated PP/PA6/PP-g-MA 80/20/5 alloys melted at various temperatures as the order marked in the curve.

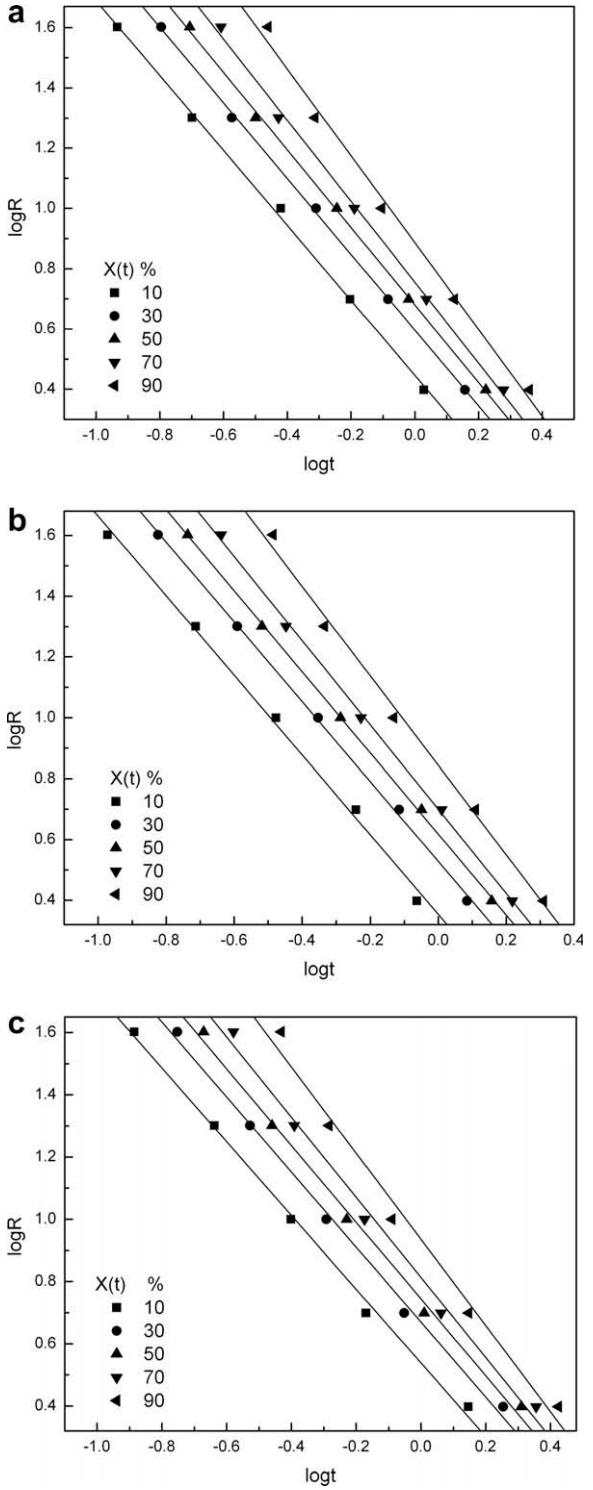

Fig. 10. (a) Plots of log *R* vs. log *t* for β-nucleated PP, (b) PP in β-nucleated PP/PA6 80/20 alloy uncompatibilized and (c) compatibilized with PP-g-MA (5 phr).

distribution of β-nucleating agent in the both phases. In order to obtain the alloy rich in β-PP with the second polar component, it is very necessary to add the compatibilizer into the alloy or to prepare it under special conditions to promote the distribution of β-nucleating agent in PP phase.

Table 3
Non-isothermal crystallization kinetic parameters of β-nucleated PP/PA6 alloy

$X(t)$ (%)		10	30	50	70	90
β-Nucleated PP	$F(t)$	2.79	3.95	4.78	5.69	7.70
	α	1.24	1.26	1.29	1.34	1.44
β-Nucleated PP/PA6 80/20	$F(t)$	2.26	3.37	4.15	5.01	6.98
	α	1.31	1.31	1.33	1.38	1.47
β-Nucleated PP/PA6/PP-*g*-MA 80/20/5	$F(t)$	3.45	4.67	5.54	6.50	8.62
	α	1.18	1.20	1.23	1.29	1.38

3.5. Non-isothermal crystallization kinetics analysis

The most commonly used isothermal crystallization kinetic equation is the well-known Avrami equation [31]. The application of this model to non-isothermal conditions was solved by Ozawa and Liu et al. [32,33]. There are several other approximations which deal with nonisothermal crystallization kinetics. A review paper of Di Lorenzo and Silvestre [34] discussed the most important non-isothermal crystallization kinetic models. The double logarithmic form of Avrami equation is [31]:

$$\log[-\ln(1 - X(T))] = \log Z_t + n\log t \quad (2)$$

where $X(T)$ is the relative crystallinity at the crystallization time t; Z_t and n are crystallization kinetic constant and Avrami exponent, respectively, and both are related to the rate and mechanism of crystallization.

Ozawa derived an equation which double logarithmic form is [32]:

$$\log[-\ln(1 - X(T))] = \log K(T) - m\log R \quad (3)$$

where R is the cooling rate, $K(T)$ is a function related to the overall crystallization rate; m is the Ozawa index, which is somewhat similar to the Avrami exponent and depends on the type of nucleation and growth dimensions.

Liu and co-workers [33] proposed a different equation by combining the Avrami and Ozawa equations, giving rise to the relationship between cooling rate R and crystallization time t at a given relative crystallinity:

$$\log Z_t + n\log t = \log K(T) - m\log R \quad (4)$$

$$\log R = \log F(T) - \alpha\log t \quad (5)$$

where the kinetic parameter, $F(T) = [K(T)/Z_t]^{1/m}$. $F(T)$ has a definite physical and practical meaning, the smaller the value of $F(T)$ is, the higher the crystallization rate becomes. The Mo exponent α is the ration of the Avrami exponent n to the Ozawa exponent m, that is, $\alpha = n/m$.

After fitting our experimental results to Ozawa equation and Mo's method, we found only Mo's method can satisfactorily describe the non-isothermal crystallization behavior of the researched alloys. At a given relative crystallinity, plots of log R against log t of β-nucleated PP, PP in β-nucleated PP/PA6 alloy and β-nucleated PP/PA6 alloy compatibilized with PP-*g*-MA are given in Fig. 10. Obviously, the plots are straight lines, implying agreement of the experimental results with Mo's theoretical prediction. The values of $F(T)$ and α can be obtained from the slopes and intercepts of the straight lines, respectively, tabulated in Table 3. For each specimen, $F(T)$ increased systematically with increasing the relative degree of crystallinity and the values of α increased slightly. However, at the same $X(T)$, the values of $F(T)$ for these specimen ranked as: β-nucleated PP/PA6/PP-*g*-MA > β-nucleated PP > β-nucleated PP/PA6. This means that to reach the same $X(T)$, the crystallization time needed of β-nucleated PP/PA6/PP-*g*-MA is the longest and that of β-nucleated PP/PA6 is the shortest. It is interesting that the crystallization time of PP in β-PP/PA6 alloy compatibilized with PP-*g*-MA is longer than that of uncompatibilized β-PP/PA6 alloy. It is attributed that the crystallization tendency of PP decreases in the presence of PP-*g*-MA, which is relative to the decreased regularity of the chains due to the modification by maleic anhydride units [23]. What's more, PP-*g*-PA6 generated by the chemical reaction between the functional group of PP-*g*-MA and the terminal groups of PA6 restricted the crystallization of PP. The shortest crystallization time of PP in β-PP/PA6 alloy is attributed that PA6 also has a nucleating effect on PP. Although the nucleating effect of PA6 is benefit for formation of α-PP, it can still accelerate PP crystallization. These results were in agreement with the crystallization behavior and polymorphic composition discussed above.

4. Conclusion

(1) Addition of PA6 into non-nucleated PP shifts the crystallization temperature of PP in PP/PA6 alloys to high temperature due to the α-nucleating effect of PA6, but it has no obvious effects on the crystallization temperature of PP in the β-nucleated PP/PA6 alloys.
(2) The β-PP content in the β-nucleated PP/PA6 alloy decreases with increasing the PA6 content. Addition of PP-*g*-MA used as compatibilizer increases the β-PP content in the alloy. The β-PP content and the crystallization temperature of PP in the compatibilized alloys are not obviously influenced by the PA6 content.
(3) The melting temperatures have a great effect on the β-PP content in both compatibilized and uncompatibilized β-nucleated PP/PA6 alloys. The increase in the melting temperature increases the β-PP content.
(4) The nucleating agent mainly distributed in the PA6 phase and/or the interface between PP and PA6 phase when blended at high temperature, which was supported by the fact that the β-PP content almost keeps constant in β-nucleated PP but decreases obviously in β-nucleated PP/PA6 alloys etched with sulfuric acid.

(5) The non-isothermal crystallization process of β-nucleated PP, PP in β-nucleated PP/PA6 alloy and PP-*g*-MA compatibilized β-nucleated PP/PA6 alloy can be successfully described by Mo's method.

Acknowledgements

The Project was supported by National Natural Science Foundation of People's Republic of China. (Grant No. 50873115).

References

[1] Varga J. β-Modification of isotactic polypropylene: preparation, structure, processing, properties, and application. J Macromol Sci Phys 2002;41(4–6):1121–71.
[2] Grein C. Toughness of neat, rubber modified and filled β-nucleated polypropylene: from fundamentals to applications. Adv Polym Sci 2005;188:43–104.
[3] Kotek J, Raab M, Baldrian J, Grellmann WJ. The effect of specific β-nucleation on morphology and mechanical behavior of isotactic polypropylene. J Appl Polym Sci 2002;85(6):1174–84.
[4] Chen HB, Karger-Kocsis J, Wu JS, Varga J. Fracture toughness of α- and β-phase polypropylene homopolymers and random- and block-copolymers. Polymer 2002;43(24):6505–14.
[5] Raab M, Sčudla J, Kolařík J. The effect of specific nucleation on tensile mechanical behaviour of isotactic polypropylene. Eur Polym J 2004;40(7):1317–23.
[6] Menyhárd A, Varga J, Molnár G. Comparison of different β-nucleators for isotactic polypropylene, characterisation by DSC and temperature-modulated DSC (TMDSC) measurements. J Therm Anal Calorim 2006;83(3):625–30.
[7] Feng J, Chen M. Effects of Lan^{3+}-containing additive on crystalline characteristics of isotactic polypropylene. Polym Int 2003;52(1):42–5.
[8] Shi G, Zhang X. Effect of β-nucleator content on the crystallization and melting behaviour of β-crystalline phase polypropylene. Thermochim Acta 1992;205:235–43.
[9] Mohmeyer N, Schmidt HW, Kristiansen PM, Altstädt V. Influence of chemical structure and solubility of bisamide additives on the nucleation of isotactic polypropylene and the improvement of its charge storage properties. Macromolecules 2006;39(17):5760–7.
[10] Meille SV, Ferro DR, Bruckner S, Lovinger AJ, Padden FJ. Structure of β- isotactic polypropylene: a long-standing structural puzzle. Macromolecules 1994;27(9):2615–22.
[11] Lovinger AJ. Microstrucure and unit-cell orientation in α-polypropylene. J Polym Sci B Polym Phys 1983;21(1):97–110.
[12] Moitzi J, Skalicky P. Shear-induced crystallization of isotactic polypropylene melts: isothermal WAXS experiments with synchrotron radiation. Polymer 1993;34(15):3168–72.
[13] Somani RH, Hsiao BS, Nogales A, Srinivas S, Tsou AH, Sics I, et al. Structure development during shear flow-induced crystallization of iPP: *in situ* small-angle X-ray scattering study. Macromolecules 2000;33(25):9385–93.
[14] Somani RH, Hsiao BS, Nogales A, Fruitwala H, Srinivas S, Tsou AH. Structure development during shear flow induced crystallization of iPP: *in situ* wide-angle X-ray diffraction study. Macromolecules 2001;34(17):5902–9.
[15] Huo H, Jiang SC, An LJ, Feng JC. Influence of shear on crystallization behavior of the beta phase in isotactic polypropylene with β-nucleating agent. Macromolecules 2004;37(7):2478–83.
[16] Zhang RH, Shi D, Tjong SC, Li RKY. Study on the β to α transformation of polypropylene crystals in compatibilized blend of polypropylene/polyamide-6. J Polym Sci B Polym Phys 2007;45(19):2674–81.
[17] Feng M, Gong FL, Zhao CG, Chen GM, Zhang SM, Yang MS, et al. The β-crystalline form of isotactic polypropylene in blends polypropylene and polyamide 6/clay nanocomposites. J Polym Sci B Polym Phys 2004;42(18):3428–38.
[18] Varga J. β-Modification of polypropylene and its two component systems. J Therm Anal 1989;35(6):1891–912.
[19] Varga J, Garzó G. The properties of polymer blends of β-modification of polypropylene and an elastomer. Angew Makromol Chem 1990;180:15–33.
[20] Shi G. Recent studies on β-crystalline form of isotactic polypropylene. In: Ghiggino KP, editor. Progress in Pacific polymer science, vol. 3. Berlin: Springer Verlag; 1994. p. 259–69.
[21] Varga J, Menyhárd A. Crystallization, melting and structure of polypropylene/poly(vinylidene-fluoride) blends. J Thermal Anal Calorim 2003;73(3):735–43.
[22] Menyhárd A, Varga J, Liber A, Belina G. Polymer blends based on the β-modification of polypropylene. Eur Polym J 2005;41(4):669–77.
[23] Menyhárd A, Varga J. The effect of compatibilizers on the crystallization, melting and polymorphic composition of β-nucleated isotactic polypropylene and polyamide 6 blends. Eur Polym J 2006;42(12):3257–68.
[24] Bartczak Z, Galeski A, Krasnikova NP. Primary nucleation and spherulite growth rate in isotactic polypropylene blends. Polymer 1987;28(10):1627–34.
[25] Bartczak A, Martuscelli E, Galeski A. Primary spherulitic nucleation in polypropylene-based blends and copolymers. In: Karger-Kocsis J, editor. Polypropylene: structure, blends and composites, vol. 2. London: Chapman and Hall; 1995. p. 25–49.
[26] Shangguan Y, Song Y, Peng M, Li B, Zheng Q. Formation of β-crystal from nonisothermal crystallization of compression-molded isotactic polypropylene melt. Eur Polym J 2005;41(8):1766–71.
[27] Turner-Jones A, Aizlewood JM, Beckett DR. Crystalline forms of isotactic polypropylene. Makromol Chem 1964;75:134–58.
[28] Ohlsson B, Hassander H, Tornell B. Improved compatibility between polyamide and polypropylene by the use of maleic anhydride grafted SEBS. Polymer 1998;39(26):6705–14.
[29] Roeder J, Oliveira RVB, Goncalves MC, Soldi V, Pires ATN. Polypropylene/polyamide-6 blends: influence of compatibilizing agent on interface domains. Polym Test 2002;21(7):815–21.
[30] Fillon B, Wittmann JC, Lotz B, Thierry A. Self-nucleation and recrystallization of isotactic polypropylene (α phase) investigated by differential scanning calorimetry. J Polym Sci B Polym Phys 1993;31(10):1383–93.
[31] Avrami M. Kinetics of phase change II: transformationtime relations for random distribution of nuclei. J Chem Phys 1940;8:212–24.
[32] Ozawa T. Kinetics of non-isothermal crystallization. Polymer 1971;12(3):150–8.
[33] Liu TX, Mo ZS, Wang SE, Zhang HF. Nonisothermal melt and cold crystallization kinetics of poly(aryl ether ether ketone ketone). Polym Eng Sci 1997;37(3):568–75.
[34] Di Lorenzo ML, Silvestre C. Non-isothermal crystallization of polymers. Prog Polym Sci 1999;24:917–50.